THE ASTROPHYSICAL JOURNAL, 552:L35–L38, 2001 May 1

GAMMA-RAY BURST AFTERGLOW WITH CONTINUOUS ENERGY INJECTION: SIGNATURE OF A HIGHLY MAGNETIZED MILLISECOND PULSAR

BING ZHANG AND PETER MÉSZÁROS
Department of Astronomy and Astrophysics, Pennsylvania State University, 525 Davey Laboratory, University Park, PA 16802
Received 2000 November 3; accepted 2001 March 20; published 2001 April 16

ABSTRACT

We investigate the consequences of a continuously injecting central engine on the gamma-ray burst afterglow emission, focusing more specifically on a highly magnetized millisecond pulsar engine. For initial pulsar parameters within a certain region of the parameter space, the afterglow light curves are predicted to show a distinctive achromatic bump feature, the onset and duration of which range from minutes to months, depending on the pulsar and the fireball parameters. The detection of, or upper limits on, such features would provide constraints on the burst progenitor and on magnetar-like central engine models. An achromatic bump such as that in the GRB 000301C afterglow may be caused by a millisecond pulsar with $P_0 = 3.4$ ms and $B_p = 2.7 \times 10^{14}$ G.

Subject headings: gamma rays: bursts — pulsars: general — radiation mechanisms: nonthermal — shock waves — stars: magnetic fields

1. INTRODUCTION

Much of the current research on gamma-ray bursts (GRBs) is aimed at determining the nature of the central engine and its progenitor system. While recently substantial results have begun to accumulate, the evidence is still tentative. Thus, the investigation of criteria to differentiate between various central engine possibilities is desirable. Almost all the present fireball models, including those considering various nonuniform injection scenarios, assume that the energy injection into the fireball occurs in a short period of time. This is also the case in the "refreshed shock" scenario (Rees & Mészáros 1998; Kumar & Piran 2000; Sari & Mészáros 2000). However, in some types of central engines, such as a fast-rotating high-field pulsar (magnetar) or a black hole plus a long-lived debris torus system, a significant energy input into the fireball may in principle continue for a timescale significantly longer than the gamma-ray emission. Therefore, there is a need to investigate a continuously fed fireball in more detail. An additional motivation is provided by the recent detection of Fe features in the X-ray afterglow of GRB 991216 after about 1.5 days (Piro et al. 2000) and GRB 000214 after about 1 day (Antonelli et al. 2000), which may require a continuing postburst outflow in order to achieve less restrictive Fe abundance constraints (Rees & Mészáros 2000). Dai & Lu (1998a, 1998b) first considered continuous injection from a millisecond pulsar to interpret the afterglow light curves of some GRBs but did not perform a systematic study on this topic. In this Letter, we investigate the observational consequences of a continuously injecting central engine, and, more specifically, we focus on the possibility that the central engine is a millisecond pulsar, in particular a highly magnetized pulsar or magnetar.

2. CONTINUOUS INJECTION DYNAMICS

We consider an engine that emits both an initial impulsive energy input $E_{\rm imp}$ as well as a continuous luminosity, the latter varying as a power law in the emission time. In this case, a self-similar blast wave is expected to form at late times (Blandford & McKee 1976). The differential energy conservation relation for the self-similar blast wave can be written as $dE/dt = \mathcal{L}_0(t/t_0)^{q'} - \kappa'(E/t)$, where E and t are the energy and time measured in the fixed frame. The first term $\mathcal{L} = \mathcal{L}_0(t/t_0)^{q'}$, where q' and κ' are dimensionless constants, denotes the continuous luminosity injection, and the second term takes into account radiative energy losses in the blast wave. For $q' \neq -1 - \kappa'$, an analytical solution is $E = [L_0/(\kappa' + q' + 1)]\,(t/t_0)^{q'}\,t + E_{\rm imp}\,(t/t_0)^{-\kappa'}$ for $t > t_0$ (Cohen & Piran 1999). Here t_0 is a characteristic timescale for the formation of a self-similar solution, which is roughly equal to the time for the external shock to start to decelerate, and $E_{\rm imp}$ is a constant that describes the impulsive energy input when $q' > -1 - \kappa'$. This is obtained under the assumption that a self-similar solution exists at $t > t_0$; hence, it cannot be extrapolated down to $t = 0$. For $t > t_0$, the bulk Lorentz factor of the fireball scales with time as $\Gamma^2 \propto t^{-m}$, with m and κ' connected by $\kappa' = m - 3$ (Cohen, Piran, & Sari 1998), and $m = 3$ for the adiabatic case (Blandford & McKee 1976).

In the observer frame, the time T is related to the fixed frame t (for which $dr = c\,dt$) by $dT = (1 - \beta)dt \simeq dt/2\Gamma^2$, and $T = \int_0^t (2\Gamma^2)^{-1}dt \simeq t/[2(m + 1)\Gamma^2]$ when $t \gg t_0$. The differential energy conservation relation can be now expressed as $dE/dT = L_0(T/T_0)^q - \kappa(E/T)$, and the integrated relation is

$$E = \frac{L_0}{\kappa + q + 1}\left(\frac{T}{T_0}\right)^q T + E_{\rm imp}\left(\frac{T}{T_0}\right)^{-\kappa}, \quad T > T_0. \qquad (1)$$

Here $L = L_0(T/T_0)^q$ is the intrinsic luminosity of the central engine, $T_0 = t_0/[2(m' + 1)\Gamma^2(t_0)]$, where m' is the self-similar index for $t < t_0$ (usually $m' = 0$ for the coasting phase), $L_0 = 2\Gamma^2(t_0)\mathcal{L}_0$, $q = (q' - m)/(m + 1)$, and $\kappa = \kappa'/(m + 1)$. Since $\kappa + q + 1 = (\kappa' + q' + 1)/(m + 1)$, the comparisons between q and $-1 - \kappa$ in the following discussions are equivalent to the comparisons between q' and $-1 - \kappa'$ (Cohen & Piran 1999). Setting $T = T_0$, the total energy at the beginning of the self-similar expansion is the sum of two terms, $E_0 = L_0T_0/(\kappa + q + 1) + E_{\rm imp}$. The first term, for $q > -1 - \kappa$, is the accumulated energy from the continuous injection (with radiative corrections) before the self-similar solution starts (note that for $q < -1 - \kappa$, the two terms no longer have a clear physical meaning since the first one is negative). The second term, $E_{\rm imp}$, is the energy injected impulsively by the initial event.

At different times, the total energy of the blast wave given by equation (1) may be dominated either by the continuous

injection term ($\propto T^{(q+1)}$) or by the initial impulsive term ($\propto T^{-\kappa}$). Which of these two is dominant at a particular observation time T depends both on the relative values of the two indices ($q+1$ and $-\kappa$; Cohen & Piran 1999) *and* on the values of L_0 and $E_{\rm imp}$ (Dai & Lu 1998a, 1998b). We then have three regimes: (1) If $q<-1-\kappa$, the second term in equation (1) always dominates since the first term is negative. The fireball is then completely analogous to the impulsive injection case. (2) If $q=-1-\kappa$, the solution in equation (1) is no longer valid, and there is no self-similar solution. (3) If $q>-1-\kappa$, the first term in equation (1) will eventually dominate over the second term after a critical time T_c, and it is this term that will exert a noticeable influence on the GRB afterglow light curves. This latter case is of the most interest here.

For a fireball blast wave decelerated by a homogeneous external medium with particle number density n, the energy conservation equation at time $t=r/c$ is

$$E=\frac{4\pi}{3}r^3nm_pc^2\Gamma^2=\frac{4\pi}{3}(ct)^3nm_pc^2\Gamma^2,\quad t>t_0, \qquad (2)$$

where r is the radius of the blast wave and all other symbols have their usual meanings. This relation holds also for more general cases with a nonconstant E. For the continuous injection–dominated case, the energy E in equation (2) should have the same time dependence as the first term on the right-hand side of equation (1), giving $T^{q+1}\propto t^3\Gamma^2$, or

$$m=\frac{2-q}{2+q},\quad q>-1-\kappa. \qquad (3)$$

Since, in general, $\Gamma\propto t^{-m/2}\propto r^{-m/2}\propto T^{-m/2(m+1)}$ and $r\propto T^{1/(m+1)}$, using equation (3), the dynamics of the continuous injection–dominated case is

$$\Gamma\propto r^{-(2-q)/2(2+q)}\propto T^{-(2-q)/8},\quad r\propto T^{(2+q)/4}. \qquad (4)$$

For such a continuously fed fireball, a forward shock propagating into the external medium and a reverse shock propagating back into the relativistic fireball will coexist on either side of the contact discontinuity. The latter may persist as long as a significant level of energy injection is going on. The radiation spectra from these shocks are complicated by many factors. Here we address only the simplest case of the standard adiabatic external shock afterglow scenario and assume that the reverse shock is mildly relativistic, as in the refreshed shock scenario. Following Mészáros & Rees (1997), Kumar & Piran (2000), and Sari & Mészáros (2000), one can work out the relationship between the temporal index α and the spectral index β, where $F_\nu\propto T^\alpha\nu^\beta$. For the forward shock, the synchrotron peak frequency $\nu_m^f\propto\Gamma B'\gamma_m^2\propto\Gamma^4\propto T^{-2m/(m+1)}\propto T^{-(2-q)/2}$, and the peak flux $F_{\nu_m}^f\propto(t^2\Gamma^5)(n_e'B'r/\Gamma)\propto T^3\Gamma^8\propto T^{(3-m)/(1+m)}\propto T^{1+q}$, so that $\alpha^f=(2m\beta^f+3-m)/(1+m)=(1-q/2)\beta^f+1+q$. For the reverse shock, $\nu_m^r=\nu_m^f/\Gamma^2\propto\Gamma^2\propto T^{-m/(m+1)}\propto T^{-(2-q)/4}$, and $F_{\nu_m}^r=\Gamma F_{\nu_m}^f\propto T^3\Gamma^9\propto T^{(6-3m)/2(1+m)}\propto T^{(6+9q)/8}$, so that $\alpha^r=(2m\beta^r+6-3m)/2(1+m)=[(4-2q)\beta^r+9q+6]/8$. At any time, the emission at a given frequency may be dominated by either the forward or the reverse shock. The above scalings are derived for the slow-cooling regime (Sari, Piran, & Narayan 1998), which is usually satisfied. The fast cooling will change the scaling laws but does not change the qualitative "index switching" picture proposed in this Letter. All the above scalings reduce to the standard adiabatic case by setting $m=3$ and $q=-1$.

The injection-dominated regime begins at a critical time T_c defined by equating the injection and energy-loss terms in equation (1),

$$T_c=\mathrm{Max}\left\{1,\left[(\kappa+q+1)\frac{E_{\rm imp}}{L_0T_0}\right]^{1/(\kappa+q+1)}\right\}T_0, \qquad (5)$$

where $T_c\geq T_0$ ensures that a self-similar solution has already formed when the continuous injection law dominates. If initially the continuous injection term is more important, i.e., $L_0T_0\geq E_{\rm imp}$, then $T_c\simeq T_0$, and the dynamics is determined by the continuous injection law as soon as the self-similar profile forms. However, if initially the impulsive term dominates ($L_0T_0\ll E_{\rm imp}$), the critical time T_c after which the continuous injection becomes dominant could be much longer than T_0, depending on the ratio of $E_{\rm imp}$ and L_0T_0.

Central engines with a continuous injection may, in addition, have another characteristic timescale $\mathcal{T}$, e.g., at which the continuous injection power-law index (say, $q_1>-1-\kappa$) switches to a lower value $q_2<-1-\kappa$. It is only for $\mathcal{T}>T_c$ that the continuous injection has a noticeable effect on the afterglow light curve. Different central engines may have different values of $\mathcal{T}$. In the following, we investigate the conditions under which a continuous injection can influence the dynamics of the blast wave, and we consider the specific case of a millisecond pulsar as a central engine with a continuous injection following after the initial impulsive phase.

3. HIGHLY MAGNETIZED MILLISECOND PULSAR AS THE CENTRAL ENGINE

Although a wide range of GRB progenitors leads to a black hole–debris torus system (Narayan, Paczyński, & Piran 1992; Woosley 1993; Paczyński 1998; Mészáros, Rees, & Wijers 1999; Fryer, Woosley, & Hartmann 1999), some progenitors may lead to a highly magnetized rapidly rotating pulsar (e.g., Usov 1992; Duncan & Thompson 1992; Thompson 1994; Yi & Blackman 1998; Blackman & Yi 1998; Kluźniak & Ruderman 1998; Nakamura 1998; Spruit 1999; Wheeler et al. 2000; Ruderman, Tao, & Kluźniak 2000). During the early stages of the evolution of these objects, the luminosity decay law could be very complicated. On the longer (afterglow) timescales that we are interested in, some short-term processes, such as the decay of the differential rotation–induced toroidal magnetic field energy (Kluźniak & Ruderman 1998; Ruderman et al. 2000), are no longer important, and the energy injection into the fireball may be mainly through electromagnetic dipolar emission. The spin-down of the pulsar may also be influenced by gravitational radiation.

Assuming that the spin-down is mainly due to electromagnetic (EM) dipolar radiation and to gravitational wave (GW) radiation, the spin-down law is $-I\Omega\dot{\Omega}=(B_p^2R^6\Omega^4)/(6c^3)+(32GI^2\times\epsilon^2\Omega^6)/(5c^5)$ (Shapiro & Teukolsky 1983), where Ω and $\dot{\Omega}$ are the angular frequency and its time derivative, respectively, B_p is the dipolar field strength at the poles, I is moment of inertia, R is stellar radius, and ϵ is the ellipticity of the neutron star. This equation can be solved for Ω as a function of T, with initial conditions $\Omega=\Omega_0$ and $\dot{\Omega}=\dot{\Omega}_0$ for $T=0$. The decay solution $\Omega(T)$ includes both EM and GW losses, but the corresponding energy input into the fireball will be due to the EM dipolar emission only, i.e., $L(T)=[B_p^2R^6\Omega(T)^4]/(6c^3)$, which usually will not be a simple power law. However, at different times, the

spin-down will be dominated by one or the other loss term, and one can get approximate solutions. When EM dipolar radiation losses dominate the spin-down, we have $\Omega = \Omega_0(1 + T/\mathcal{T}_{\rm em})^{-1/2}$, or approximately $\Omega = \Omega_0$ for $T \ll \mathcal{T}_{\rm em}$, and $\Omega = \Omega_0(T/\mathcal{T}_{\rm em})^{-1/2}$ for $T \gg \mathcal{T}_{\rm em}$. Here

$$\mathcal{T}_{\rm em} = \frac{3c^3 I}{B_p^2 R^6 \Omega_0^2} = 2.05 \times 10^3 \ {\rm s}(I_{45} B_{p,15}^{-2} P_{0,-3}^2 R_6^{-6}) \quad (6)$$

is the characteristic timescale for dipolar spin-down, $B_{p,15} = B_p/(10^{15}\ {\rm G})$, and $P_{0,-3}$ is the initial rotation period in milliseconds. When GW radiation losses dominate the spin-down, the evolution is $\Omega \simeq \Omega_0(1 + T/\mathcal{T}_{\rm gw})^{-1/4}$, where $\mathcal{T}_{\rm gw} = (5c^5/128GI\epsilon^2\Omega_0^4) = 0.91\ {\rm s}[I_{45}^{-1}P_{0,-3}^4(\epsilon/0.1)^{-2}]$. GW spin-down is important only when the neutron star is born with an initial $\Omega_0 \gtrsim \Omega_* \sim 10^4\ {\rm s}^{-1}$ (e.g., Usov 1992; Blackman & Yi 1998). In such cases, the ellipticity is large ($\epsilon \sim 0.1$) because of rotational instability, and the timescale for the GW-dominated regime is short, so that Ω will be damped to below Ω_* promptly in a time $\mathcal{T}_* = [(\Omega_0/\Omega_*)^4 - 1]\mathcal{T}_{\rm gw}$. After $\Omega < \Omega_*$, GW losses decrease sharply, and the spin-down becomes dominated by the EM losses. If the neutron star is born with $\Omega_0 < \Omega_*$, the spin-down will always be in the EM regime since the typical spin-down time for GW radiation is much longer.

For these regimes, the two cases for continuous injection are as follows:

(*a*) $\Omega_0 < \Omega_*$, an EM-loss–dominated regime. In this case,

$$L(T) = L_{\rm em,0}\frac{1}{(1 + T/\mathcal{T}_{\rm em})^2} \simeq \begin{cases} L_{\rm em,0}, & T \ll \mathcal{T}_{\rm em}, \\ L_{\rm em,0}(T/\mathcal{T}_{\rm em})^{-2}, & T \gg \mathcal{T}_{\rm em}, \end{cases} \quad (7)$$

where $\mathcal{T}_{\rm em}$ is given by equation (6), and

$$L_{\rm em,0} = \frac{I\Omega_0^2}{2\mathcal{T}_{\rm em}} \simeq 1.0 \times 10^{49}\ {\rm ergs\ s^{-1}}(B_{p,15}^2 P_{0,-3}^{-4} R_6^6). \quad (8)$$

(*b*) $\Omega_0 > \Omega_*$, an initially GW-dominated regime. The continuous injection luminosity can be divided into two phases, i.e., $L = L_{\rm em,0}/(1 + T/\mathcal{T}_{\rm gw})$ for $T < \mathcal{T}_*$ or $L = L_{\rm em,*}/[1 + (T - \mathcal{T}_*)/\mathcal{T}_{\rm em,*}]^2$ for $T > \mathcal{T}_*$, where $L_{\rm em,0}$ is given by equation (8), and $L_{\rm em,*} = I\Omega_*^2/2\mathcal{T}_{\rm em,*} \simeq 1.0 \times 10^{49}\ {\rm ergs\ s^{-1}}(B_{p,15}^2 P_{*,-3}^{-4} R_6^6)$, where $\mathcal{T}_{\rm em,*} = 3c^3 I/B_p^2 R^6 \Omega_*^2 \simeq 2.05 \times 10^3\ {\rm s}(I_{45} B_{p,15}^{-2} P_{*,-3}^2 R_6^{-6})$.

The above continuous injection luminosities have, for certain times, a temporal index $q = 0 > -1$, which may dominate the blast-wave dynamics. The typical duration times for this flat injection law are $\mathcal{T}_{\rm em}$ for case *a* or $\mathcal{T}_{\rm gw}$ and $\mathcal{T}_{\rm em,*}$ for case *b*. In case *b*, there are two luminosity "plateaus." The former is usually much shorter than T_c unless a very dense medium is assumed (see below), so it is unlikely to detect such a "two-step" injection-dominated case. If Ω_* is close to Ω_0, the second timescale for case *b*, $\mathcal{T}_{\rm em,*}$, may not be much different from $\mathcal{T}_{\rm em}$. In the following, for simplicity, we discuss case *a* only, keeping in mind the possible extra complexity that case *b* may introduce in some extreme cases.

During the time interval $T_c < T < \mathcal{T}_{\rm em}$, one can expect a distinctive pulsar feature to show up in the light curve. We take as an example equation (7), setting $q = 0$ in this regime and $q = -1$ otherwise (since the second slope $q = -2$ would mimic in effect the standard impulsive $q = -1$, $m = 3$ adiabatic case). For the slow-cooling external shock scenario (§ 2), the temporal decay index changes at T_c from α_1 to $\alpha_2 = \frac{2}{3}\alpha_1 + 1$ and changes back to α_1 after $\mathcal{T}_{\rm em}$. The temporal index is related to the spectral slope β through $\alpha_1 = (3/2)\beta$ for the forward shock and $\alpha_1 = (6\beta - 3)/8$ for the reverse shock. This implies an *achromatic* bump in the light curve, which could provide a signature for a pulsar. However, not all millisecond pulsars would give such observable signatures. The condition for detecting this feature is $\mathcal{T}_{\rm em} > T_c$, which constrains the pulsar initial parameter phase space. Let us specify the pulsar case in equation (5), i.e., $q = 0$, and further assume $\kappa = 0$, so that equation (5) is simplified to $T_c = {\rm Max}\,(1, E_{\rm imp}/L_0 T_0)T_0$. This gives two possibilities:

I. E_0 is mainly due to the continuous injection, i.e., $E_{\rm imp} \lesssim L_0 T_0$. This is the case considered in many pulsar GRB central engine models (Usov 1992; Duncan & Thompson 1992; Thompson 1994; Spruit 1999). We then have $T_c = T_0$ and $E_0 \simeq L_{\rm em,0} T_0$ (a factor of 2 if the continuous injection and the prompt injection energies are comparable). Solving $E_0 = (4\pi/3)(2c\Gamma_0^2 T_0)^3 n m_p c^2 \Gamma_0^2$ (in which $m' = 0$ has been adopted), where $\Gamma_0 = \Gamma(T_0) = E_0/\Delta M c^2$ is the initial bulk Lorentz factor of the blast wave, we have $T_c = T_0 \simeq 0.33\ {\rm s}\,(B_{p,15} P_{0,-3}^{-2} R_6^3) \times (\Gamma_0/300)^{-4} n^{-1/2}$. The condition $\mathcal{T}_{\rm em} > T_0$ then implies that

$$B_{p,15} < 18.4 P_{0,-3}^{4/3} I_{45}^{1/3} R_6^{-3} (\Gamma_0/300)^{4/3} n^{1/6}. \quad (9)$$

II. E_0 is dominated by the impulsive term $E_{\rm imp}$. This could be the case if the central engine is a pulsar, the initial impulsive GRB fireball being due, e.g., to $\nu\bar{\nu}$ annihilation (e.g., Eichler et al 1989), dissipation of the initial differential rotation (Ruderman et al. 2000), phase conversion from a neutron star to a strange star (Dai & Lu 1998b), etc. In this case, since $E_{\rm imp} > L_0 T_0$, we have $T_c = E_{\rm imp}/L_{0,\rm em} = (2E_{\rm imp}/I\Omega_0^2)\mathcal{T}_{\rm em}$. The condition $\mathcal{T}_{\rm em} > T_c$ is simply $E_{\rm imp} < \frac{1}{2} I\Omega_0^2$, or

$$P_{0,-3} < 4.4 I_{45}^{1/2} E_{\rm imp,51}^{-1/2}. \quad (10)$$

Since both $\mathcal{T}_{\rm em}$ and T_c are large in this case, the continuous injection term may dominate at a later time. An additional constraint, to avoid rotational breakup of the pulsar, is

$$P_0 > P_0({\rm min}). \quad (11)$$

Equations (9), (10), and (11) define a region of the pulsar P_0, $B_{p,0}$ initial parameter space (see Fig. 1) inside which the continuous injection has the observational signature discussed above, i.e., a bump in the light curve. The separation between the two regimes is defined by the condition $L_{\rm em,0} T_0 \simeq 10^{51} E_{\rm imp,51}$ ergs, or $B_{p,15} \simeq 6.7 P_{0,-3}^2 R_6^{-3} (\Gamma_0/300)^{4/3} n^{1/6} E_{\rm imp,51}^{1/3}$. Above this line (regime I), $T_c \sim T_0$, and one expects only one change, starting with the flat regime and changing to steep; below this line (regime II), one expects two changes, starting with the steep decay and followed by a flat regime and a final resumption of the steep decay.

4. DISCUSSION

If the central engines of GRBs are fast-rotating pulsars, the afterglow light curves may show a distinctive, achromatic feature for pulsars whose initial parameters are within the "pulsar signature" region defined by equations (9), (10), and (11). In this case, the afterglow light curves flatten after a critical time T_c (eq. [5]) and steepen again after a time $\mathcal{T}_{\rm em}$ (eq. [6]). This region of pulsar parameter phase space includes "magnetars"

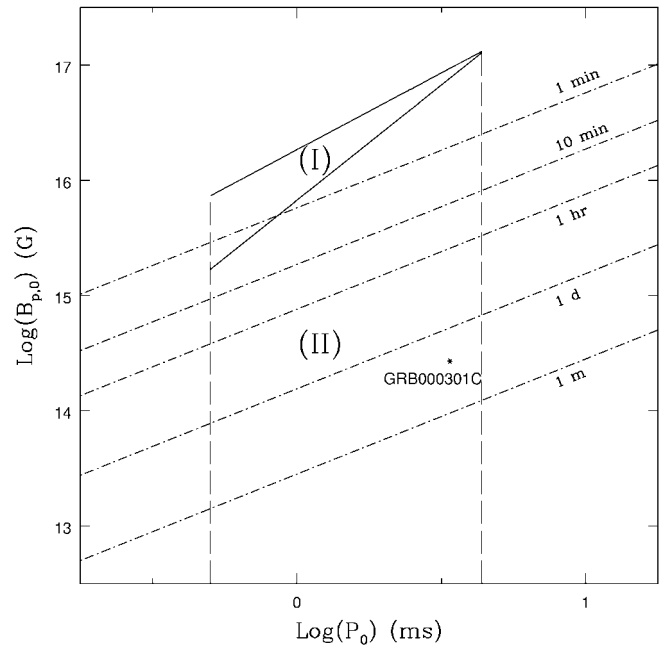

FIG. 1.—B_p-P_0 diagram for the initial parameters of a pulsar born in a GRB. The enclosed areas (regimes I and II) are the phase spaces where an achromatic pulsar signature is expected in the GRB afterglow light curves. The dot-dashed lines denote various $T_{\rm em}$ expected. $E_{\rm imp} = 10^{51}$ ergs s^{-1}, $\Gamma_0 = 300$, $n = 1$ cm^{-3}, and P_0(min) = 0.5 ms have been adopted.

or ultrahigh-field pulsars, which play a large role in some GRB pulsar progenitor models.

The current data on early afterglows are insufficient to provide good tests for this feature. However, an interesting possibility is the achromatic bump observed in the afterglow of GRB 000301C, which for a limited time deviates significantly from the standard broken power-law fit (Masetti et al. 2000). Possible explanations include running into a nonuniform ambient density (Berger et al. 2000) and modification by a microlensing event (Garnavich, Loeb, & Stanek 2000). We suggest here a third possibility, that the bump may be caused by the pulsar signature discussed above. Taking (Berger et al. 2000) $\alpha_1 \sim -1.28$ for the principal temporal index (before the bump and before the decay ascribed to a jet transition), the temporal index during the pulsar signature is expected to be $\alpha_2 \sim 0.15$, which seems reasonable for fitting the achromatic bump. Since the feature occurs a couple of days after the GRB trigger, the initial pulsar parameters are in regime II. Taking $E_{\rm imp,\,51} \sim 1.1$ from the observations (Berger et al. 2000), the pulsar parameters follow from setting $T_{\rm em} \sim 3.8$ days and $T_c \sim 2.5$ days, which gives $P_0 \sim 3.4$ ms and $B_{p,\,15} \sim 0.27$ (Fig. 1). A detailed χ^2 fit to the data would be necessary to validate this proposal.

Another relevant observation may be the recent Fe line detection in the X-ray afterglow of GRB 991216 (Piro et al 2000), which in one interpretation would require a continuously injecting central engine (Rees & Mészáros 2000). If $L_{\rm em} \sim 10^{47}$ ergs s^{-1} is assumed 37 hr after the burst (Rees & Mészáros 2000), this continued injection could be due to a pulsar with $B_{p,\,15} \sim 0.15$ and $P_0 < 1.2$ ms, which would imply a signature bump at $\gtrsim$1 hr. Such a bump is not seen in this afterglow (e.g., Halpern et al. 2000). However, a slightly weaker luminosity (e.g., $L_{\rm em} \leq 3 \times 10^{46}$ ergs s^{-1}) could also explain the Fe line features by assuming a slightly larger Fe abundance (which is very low in this model). The required pulsar can therefore be more magnetized, and the characteristic times for the signature bump would be expected early enough to have evaded detection in this GRB.

In conclusion, the detection of, or upper limits on, such characteristic afterglow bumps by missions such as *HETE-2* or *Swift* may be able to provide interesting constraints on magnetar GRB models and their progenitors.

We thank Z. G. Dai, M. J. Rees, and the referee for comments and NASA (NAG5-9192 and NAG5-9193) for support.

REFERENCES

Antonelli, L. A., et al. 2000, ApJ, 545, L39
Berger, E., et al. 2000, ApJ, 545, 56
Blackman, E. G., & Yi, I. 1998, ApJ, 498, L31
Blandford, R., & McKee, C. 1976, Phys. Fluids, 19, 1130
Cohen, E., & Piran, T. 1999, ApJ, 518, 346
Cohen, E., Piran, T., & Sari, R. 1998, ApJ, 509, 717
Dai, Z. G., & Lu, T. 1998a, A&A, 333, L87
———. 1998b, Phys. Rev. Lett., 81, 4301
Duncan, R. C., & Thompson, C. 1992, ApJ, 392, L9
Eichler, D., Livio, M., Piran, T., & Schramm, D. N. 1989, Nature, 340, 126
Fryer, C., Woosley, S., & Hartmann, D. 1999, ApJ, 526, 152
Garnavich, P., Loeb, A., & Stanek, K. 2000, ApJ, 544, L11
Halpern, J. P., et al. 2000, ApJ, 543, 697
Kluźniak, W., & Ruderman, M. 1998, ApJ, 505, L113
Kumar, P., & Piran, T. 2000, ApJ, 532, 286
Masetti, N., et al. 2000, A&A, 359, L23
Mészáros, P., & Rees, M. J. 1997, ApJ, 476, 232
Mészáros, P., Rees, M. J., & Wijers, R. 1999, NewA, 4, 303
Nakamura, T. 1998, Prog. Theor. Phys., 100, 921
Narayan, R., Paczyński, B., & Piran, T. 1992, ApJ, 395, L83
Paczyński, B. 1998, ApJ, 494, L45
Piro, L., et al. 2000, Science, 290, 955
Rees, M. J., & Mészáros, P. 1998, ApJ, 496, L1
———. 2000, ApJ, 545, L73
Ruderman, M., Tao, L., & Kluźniak, W. 2000, ApJ, 542, 243
Sari, R., & Mészáros, P. 2000, ApJ, 535, L33
Sari, R., Piran, T., & Narayan, R. 1998, ApJ, 497, L17
Shapiro, S. L., & Teukolsky, S. A. 1983, Black Holes, White Dwarfs, and Neutron Stars: The Physics of Compact Objects (New York: Wiley)
Spruit, H. C. 1999, A&A, 341, L1
Thompson, C. 1994, MNRAS, 270, 480
Usov, V. V. 1992, Nature, 357, 472
Wheeler, J. C., Yi, I., Höflich, P., & Wang, L. 2000, ApJ, 537, 810
Woosley, S. E. 1993, ApJ, 405, 273
Yi, I., & Blackman, E. G. 1998, ApJ, 494, L163